

(This is a sample cover image for this issue. The actual cover is not yet available at this time.)

This article appeared in a journal published by Elsevier. The attached copy is furnished to the author for internal non-commercial research and education use, including for instruction at the authors institution and sharing with colleagues.

Other uses, including reproduction and distribution, or selling or licensing copies, or posting to personal, institutional or third party websites are prohibited.

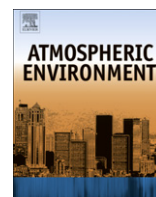
In most cases authors are permitted to post their version of the article (e.g. in Word or Tex form) to their personal website or institutional repository. Authors requiring further information regarding Elsevier's archiving and manuscript policies are encouraged to visit:

<http://www.elsevier.com/copyright>



Contents lists available at SciVerse ScienceDirect

## Atmospheric Environment

journal homepage: [www.elsevier.com/locate/atmosenv](http://www.elsevier.com/locate/atmosenv)

## Short communication

## Particle emission from laser printers with different printing speeds

Jeong Hoon Byeon<sup>a</sup>, Jang-Woo Kim<sup>b,\*</sup><sup>a</sup> Department of Chemistry, Purdue University, IN 47907, United States<sup>b</sup> Department of Digital Display Engineering, Hoseo University, Asan 336-795, Republic of Korea

## ARTICLE INFO

## Article history:

Received 21 December 2011

Accepted 1 February 2012

## Keywords:

Particle emission

Laser printers

Printing speed

Coagulation

## ABSTRACT

The present work investigated particle emissions for 10 min operating time for commercial color laser printers having different printing speeds (5, 24, 38 prints per minute (ppm)) in an experimental chamber (5 m<sup>3</sup>) under 1 h<sup>-1</sup> of air exchange rate. Number and mass concentrations of the emission particles were measured, and a correlation between emission and printing speed is discussed. The average mobility equivalent particle diameter (50–244 nm) of the emission was proportional to the printing speed (5–38 ppm) but the average particle number concentration ( $5.3\text{--}1.2 \times 10^4$  particles cm<sup>-3</sup>) was inversely proportional to the speed. From morphology analyses of the particles, it could be estimated that the number decrease (or diameter increase) rates of the primary particles due to coagulation were 3.25 (0.17), 3.40 (0.44), and  $9.31 \times 10^3$  (0.96) particles cm<sup>-3</sup> s<sup>-1</sup> (nm s<sup>-1</sup>) for 5, 24, and 38 ppm, respectively. Corresponding particle mass emission rates (or mass emission per print) were 0.007 (0.23), 0.039 (0.27), and 0.449 (1.97) mg h<sup>-1</sup> ( $\times 10^{-4}$  mg print<sup>-1</sup>) for 5, 24, and 38 ppm, respectively.

© 2012 Elsevier Ltd. All rights reserved.

## 1. Introduction

Computers, printers, copiers and other electronic equipment are a common part of the home and office environments. Different types of home or office printing devices have been used to an ever-increasing degree since their first commercial introduction (Lee et al., 2001). An electrophotographic system is one of the most common printing techniques, and widely used for laser printers and photocopiers (Chen and Chiu, 2008). The requests for improvement of the printing technology, such as high speed, high quality, downsizing, high stability, low cost, energy saving, environmental friendliness, and so on, increase more and more with the rapid development of information technologies in the past decade (Mio et al., 2009).

Airborne particles in indoor environments are considered to be an important factor due to various health effects and also for how inhabitants perceive the environment (Gudmundsson et al., 2007). Laser printers are widely used in occupational settings (Hänninen et al., 2010), but an indoor source of fine airborne particles which has recently come to attention is the use of laser printers for home or office use (Kagi et al., 2007). Previous studies (He et al., 2007; Schripp et al., 2008; Wensing et al., 2008) have reported on the

emission of submicron (<1 μm)- and ultrafine (<0.1 μm)-sized particles from commercial laser printers, and more recently, the particle source (Wensing et al., 2008; Kim et al., 2009) and particle removal using commercial filters (Wensing et al., 2008) were described. There have been several studies on printer particle emissions, but it only described differences of the emission rate with different printers. It has been shown that there are potentially many factors that may affect printer emission rates and other emission characteristics including: printer model and age, cartridge type and age, as well as paper type. However, fundamental gaps in knowledge still remain, for example, it is not clear what normally makes a printer a high emitter or why some models alternate between being low and high emitters.

Nevertheless, Kim et al. (2009) reported that the particles from a laser printer mainly emitted from a toner fixation unit, the so-called a fuser, and consequently, the fuser operating condition may induce different particle size distributions from the operation of the printer. The final step in the laser printing processes is the permanent fixation of the applied toner image on the paper by the fuser. In general, fusing involves the physical-chemical mechanisms of melting of the thermoplastic base polymer(s) of the toner, followed by particle sintering or coalescence, spreading on the paper surface and penetration into its pores, prior to resolidification (Pettersson and Fogden, 2006). The condition of the fuser operation normally depends on its printing speed, and thus, this may introduce a variety of size distributions of emission particles during the

\* Corresponding author. Tel.: +82 41 540 5925; fax: +82 41 540 5929.  
E-mail address: [jwkim@hoseo.edu](mailto:jwkim@hoseo.edu) (J.-W. Kim).

printing process. On the other hand, it is impossible to satisfy all of the requests and manufacturing the new laser printer is very tough work. For example, if the newly fabricated toners or fuser systems are starting to be used for the high speed printing and/or high quality of printed images, it is difficult to control particle emissions and also optimize electrophotographic parameters. Thus, it is important to develop a better understanding of the emissions from the printers with different speeds in order to apply the emission trend into an optimization of the printer design and/or emission control.

To address this need, we have measured number and mass concentrations of the emission particles using a scanning mobility particle sizer (SMPS) and a particle mass monitor (PMM) in an experimental chamber ( $5 \text{ m}^3$ ), and a correlation between the emission and printing speed (5, 24, and 38 prints per minute (ppm)) was discussed.

## 2. Experimental

Recent measurements showed differences between the particle emissions from printers made by different manufacturers. In this work, three printers from the same manufacturer were tested to perform parametrically. Our experimental setup (a) and real image (b) are shown in Fig. 1. Commercial laser printers with different printing speeds (5, 24, 38 ppm), which were the triboelectric charging type of color printers with a modification to easily compare particle emissions were individually placed in a test chamber of  $5 \text{ m}^3$  in a volume. The 5 and 24 ppm printers contained a single-component (charging between toners) electrophotographic system while the 38 ppm printer contained a two-component (charging between toner and magnetic particle (carrier)) system. The chamber was designed using stainless steel, and the experiment was carried out in the chamber operated at

a temperature of  $23 \text{ }^\circ\text{C}$  and 50% relative humidity. Filtered air using an activated carbon bed and a high efficiency particulate air (HEPA) filter was delivered to the top of the chamber, and the air was exhausted from the bottom of the right-side of the chamber with a flow rate of  $83.5 \text{ L min}^{-1}$  (air exchange rate:  $1 \text{ h}^{-1}$  following the RAL-UZ 122 printer testing procedure for the German "Blue Angel" certification).

In testing, the printer was placed in the bottom of the chamber, and the measurements were conducted in three phases: (1) background concentration measurements were taken until the particle number concentration in the chamber was lower than  $100 \text{ particles cm}^{-3}$  and the mass concentration was lower than  $0.001 \text{ mg m}^{-3}$  (which was controlled by introducing filtered air), (2) concentration measurements were taken immediately after the print job, and (3) a measurement was taken  $\sim 240 \text{ min}$  after the print job had finished. The same brand of standard quality white paper ( $80 \text{ g m}^{-2}$ ) was used in all tests.

The number and size distribution was monitored over the entire duration of the experiment by a SMPS system consisting of a differential mobility analyzer (3081, TSI), a condensation particle counter (3025, TSI), and an aerosol charge neutralizer (Aerosol Neutralizer 4530, HCT). The SMPS system was operated with a sample flow rate of  $1.0 \text{ L min}^{-1}$ , and the concentration of particles with a mobility equivalent diameter  $15\text{--}700 \text{ nm}$  was measured. The particle mass concentration was measured using a piezobalance type PMM (3521, Kanomax). Sampled particles first became electrically charged and collected on the piezo-crystal. The total mass of the collected particles affected the frequency of the piezo-crystal. Since the change in frequency was proportional to the mass of the particles, the actual weight of the particles was obtained.

The number and size distribution and mass concentration were simultaneously measured in a time-dependent manner when the

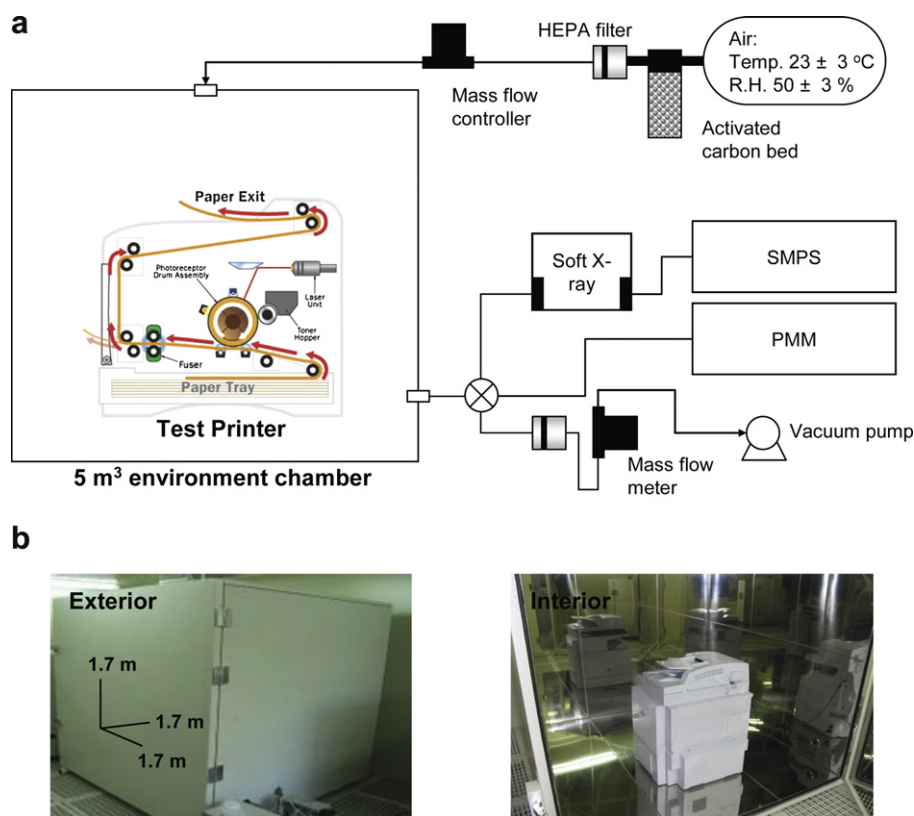


Fig. 1. (a) Schematic of the experimental setup. (b) Real image.

20% color pattern (Blue Angel RAL-UZ 122) was printed on the paper for 10 min with 5 (50), 24 (240), or 38 ppm (380 prints) of each printing speed. Experiments for each printing speed were repeated 3 times.

### 3. Results and discussion

Fig. 2a shows ppm time-dependent number and size distributions of emission particles during a 240 min time period. There was an observable increase in the concentration ( $\sim 10^4$  particles  $\text{cm}^{-3}$ ) when printing began. The increase in the particle concentration during the printing was due to the time required to fill the chamber with a sufficiently high particle concentration. For the 5 ppm case, an average particle diameter of  $\sim 45$  nm appeared when the printing was started. The following SMPS measurements showed the shift of particle diameter which became larger ( $\sim 75$  nm) while continually decreasing in magnitude (refer Fig. 2b). Changes in the distribution due to coagulation and particle size-dependent deposition were suggested. Size distribution change through particle loss to the chamber walls, such as through particle deposition due to Brownian or turbulent diffusion or due to thermal gradients (thermophoresis), were rather slow processes. For example, Bémer et al. (2002) showed that for particles  $< 5 \mu\text{m}$ , the time scale for a significant change in the particle number concentration due to turbulent diffusion was in the range of 1 h; for Brownian diffusion it was even longer. On the other hand, collisional growth, which was a function of the number concentration, could produce a significant change in size distribution within minutes or seconds during common workplace conditions. It could be concluded that a remarkable change of the size distribution during printing and

a decay of concentration after printing might be dominantly affected by coagulation and particle deposition, respectively.

Fig. 2a also shows that the size distributions of the particles emitted from the printers were monodisperse. In the presence of background particles, i.e., during the printing, the particles evolved very rapidly into a quasi-steady state. At the high end of the background concentration, almost all the primary particles vanished due to attachment onto the larger background particles (i.e., agglomerates), thus a peak of the primary particles was invisible in the size distribution depending on the coagulation rate. The coagulation rate was proportional to the square of the particle concentration and thus rose rapidly as the chamber fills, leading to coagulation and to a decrease in concentration. According to reports by Schripp et al. (2008) and Wensing et al. (2008), the rapid measurement also reported that the emission contained a remarkable amount of particles near a diameter of 10 nm. From scanning electron microscope (SEM) analyses, the measured particles in this work were mostly clusters of very small particles (i.e., primary particles,  $\sim 10$  nm; refer to insets in Table 1), and these were aged particles consisting of large, loose coagulates. Equation (1) described the change in the number concentration (or particle diameter) of primary particles as a function of collisions within the primary particles as well as collisions with background particles where the concentration is consistent with the following equation:

$$\frac{dC_{pp}}{dt} \left( \text{or } \frac{dd_{pp}}{dt} \right) \propto (K_{pp}C_{pp}^2 + K_{bp}C_{pp}C_{bp}) \quad (1)$$

where,  $C_{pp}$  and  $C_{bp}$  are the respective number concentrations of primary (measured by SEM) and background (measured by SMPS) particles,  $d_{pp}$  and  $d_{bp}$  are the diameters of the primary and

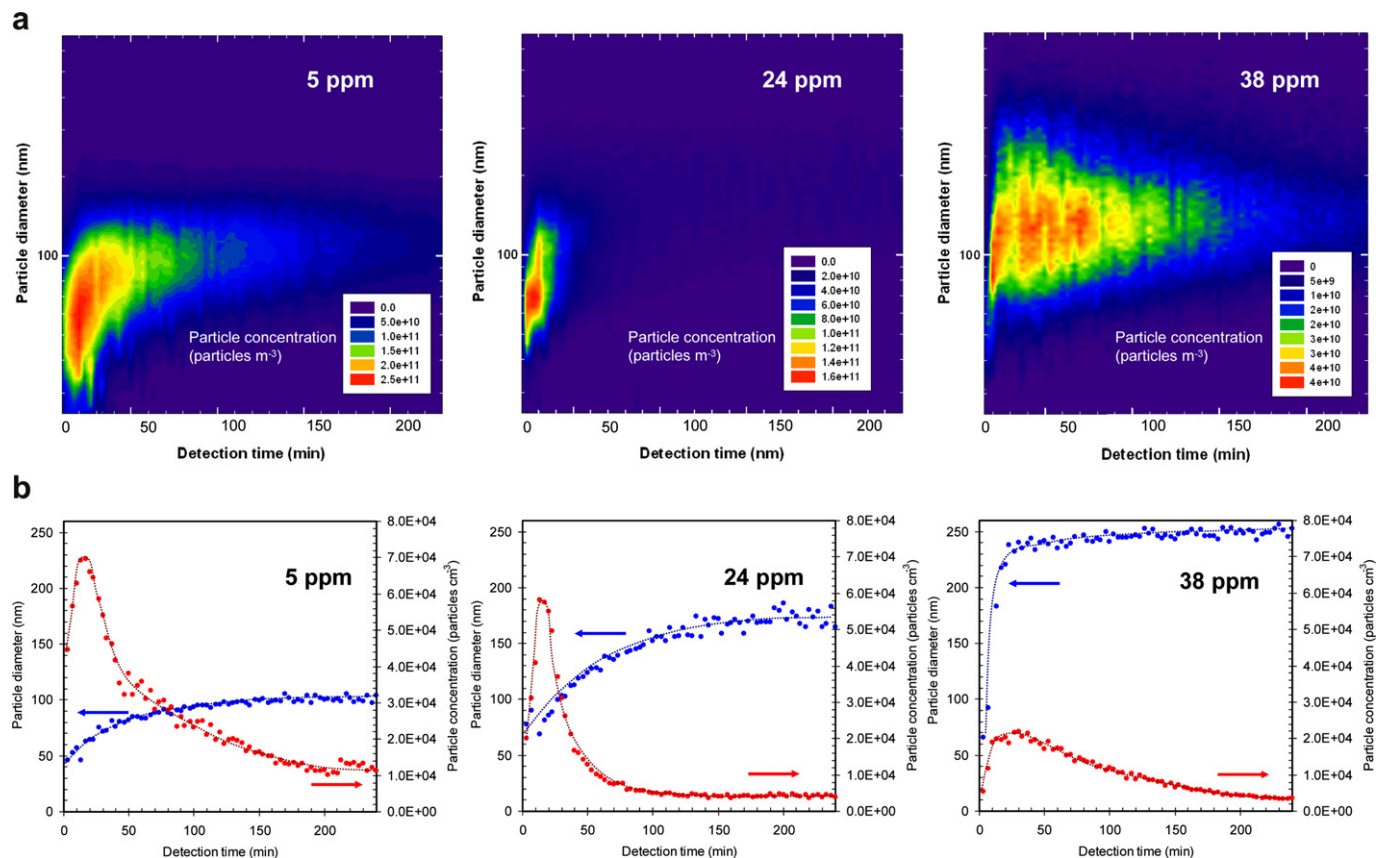
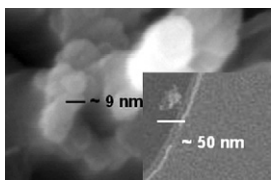
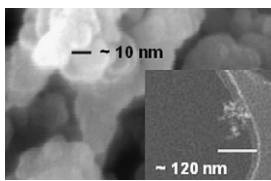


Fig. 2. Time dependent results of particle emission with different printing speeds (5: left, 24: center, and 38 ppm: right). (a) Number size distribution and (b) change of average number concentration and diameter.



**Table 1**

Changes in the number concentration and diameter of emission particles with different printing speeds.

Items	5 ppm	24 ppm	38 ppm
$d_{bp}$ (nm)			
$d_{pp}$ (nm)			
$D_f$	1.58	1.66	1.82
$n_{pp}$	15.8	56.4	191.1
$C_{bp}$ (particles $cm^{-3}$ )	$5.28 \times 10^4$	$1.47 \times 10^4$	$1.17 \times 10^4$
$C_{pp}$ (particles $cm^{-3}$ )	$0.83 \times 10^6$	$0.83 \times 10^6$	$2.24 \times 10^6$
Number concentration decrease rate (particles $cm^{-3} s^{-1}$ )	$2.71 \times 10^3$	$3.40 \times 10^3$	$9.31 \times 10^3$
Diameter increase rate (nm $s^{-1}$ )	0.17	0.44	0.96

background particles,  $K_{pp}(=\frac{4kT}{3\mu})$  and  $K_{bp}(=\frac{2kTd_{pp}}{3\mu d_{bp}})$  are the respective coagulation rate constants for homogeneous (between primary particles) and heterogeneous (between primary and background particles) collisions,  $kT$  the Boltzmann factor, and  $\mu$  the gas viscosity (Hinds, 1999). Here, the  $C_{pp}$  term was derived via the production of  $C_{bp}$  and  $n_{pp}$  (the number of primary particles in an agglomerate;  $n_{pp} = \frac{d_{bp}^{D_f}}{d_{pp}^{D_f}}$ , where  $D_f$  is the fractal dimension). The coagulation rate constants changed their size and number concentration by coagulation, homogeneously by coagulation within the particle size class or heterogeneously by interaction with the background particles (Seipenbusch et al., 2008). Details of our results are listed in Table 1. The average particle diameter was the smallest for the 5 ppm printer (50.4 nm), although it was interesting to note that the 5 ppm printer had the largest emission in number concentration ( $5.3 \times 10^4$  particles  $cm^{-3}$ ). Lesser concentrations (or larger diameters) with increasing printing speed was due to the higher coagulation rate with higher primary particle concentrations.

Finally, we estimated the average particle mass emission rates ( $R_{ame}$ ,  $mg h^{-1}$ ) with different printing speeds, and the corresponding approximation is as follows:

$$R_{ame} = m_{bp}C_{bp}Q \quad (2)$$

where  $m_{bp}$  (defined by  $m_{bp} = (\pi/6)\rho_{cor}d_{bp}^3$ , where  $\rho_{cor}$  is the correlation density between the mass concentration ( $C_{bp-m}$ ) measurements of SMPS and PMM.) is the mass of a particle with a measured average diameter  $d_{bp}$  and  $Q$  is the flow rate of the test chamber (Virtanen et al., 2004). Additionally, particle mass emissions per print ( $m_{pe-p}$ ) were estimated by dividing the mass emission rate with the printing speed. Details of the results are described in Table 2.

From the results of the number size distribution and particle mass emission (refer to Tables 1 and 2), the degree of emission was proportional to the printing speed. In high speed printers

(>30 ppm in printing speed), a fuser operation with a higher temperature ( $\leq 230$  °C) than lower-speed printers ( $\leq 200$  °C) was generally needed to promote a fast fixation of toners on paper. More severe conditions for high speed printers induced a higher rate of evaporation of toner and/or fuser materials. This resulted in a higher rate of nucleation and condensation to form primary particles, and these particles then coagulated to form agglomerates. Kim et al. (2009) indeed reported that particle emission was remarkably affected by a fusing temperature at a level of 190 °C. Moreover, for the two-component printer (38 ppm case in this work), small toner particles were mixed with larger magnetic carriers. The toner and carrier were chosen so that they exchanged electric charge and became oppositely charged when mixed (Anderson, 1996). The surface of the applied toner particles was typically coated with 10–100 nm silica particles to achieve a stable image quality. In the two-component printer, a mixture of the toner and carrier was picked up by a developer roll, metered using a trim bar to achieve a uniform thickness, and transported to the development zone where the toners were presented to the image on the photoconductor. The toner and carrier particles were repeatedly subject to mechanical stresses during the mixing, trimming, and development processes. Ramesh (2009) reported that silica particles on the toner surface mostly detached during the two-component printing processes by mechanical stresses. These detached particles might also contribute to a remarkable increase in the particle diameter and mass emission for the 38 ppm case. In addition, from energy dispersive X-ray (EDX) analyses of sampled emission particles, the 38 ppm case emitted  $\sim 2.8$  times more silicon elements than those in the 5 and 24 ppm cases.

#### 4. Concluding remarks

The number and mass concentrations of the emitted particles were respectively measured using SMPS and PMM, and a correlation between the emission and printing speed was discussed. The average mobility equivalent particle diameter (50–244 nm) during printing was proportional to the printing speed (5–38 ppm) but the average particle number concentration ( $5.3$ – $1.2 \times 10^4$  particles  $cm^{-3}$ ) was inversely proportional to the speed. From morphology analyses of the particles, it could be estimated that the rate of number decrease (or diameter increase) of primary particles due to coagulation were  $3.25$  ( $0.17$ ),  $3.40$  ( $0.44$ ), and  $9.31 \times 10^3$  ( $0.96$ ) particles  $cm^{-3} s^{-1}$  (nm  $s^{-1}$ ) for 5, 24, and 38 ppm, respectively. By correlating between mass concentrations from SMPS and PMM measurements, the average particle mass emission rates (or mass emission per print) were estimated as  $0.007$  ( $0.23$ ),  $0.039$  ( $0.27$ ), and  $0.449$  ( $1.97$ )  $mg h^{-1}$  ( $\times 10^{-4} mg print^{-1}$ ) for 5, 24, and

**Table 2**

Average mass rate of emission particles with different printing speeds.

Items	5 ppm	24 ppm	38 ppm
$\rho_{cor}$ (g $cm^{-3}$ )	0.396	0.660	1.008
$m_{bp}$ (g particles $^{-1}$ )	$0.026 \times 10^{-15}$	$0.536 \times 10^{-15}$	$7.644 \times 10^{-15}$
$C_{bp-m}$ (g $cm^{-3}$ )	$0.14 \times 10^{-11}$	$0.79 \times 10^{-11}$	$8.98 \times 10^{-11}$
$R_{ame}$ (mg $h^{-1}$ )	0.007	0.039	0.449
$m_{pe-p}$ (mg print $^{-1}$ )	$0.23 \times 10^{-4}$	$0.27 \times 10^{-4}$	$1.97 \times 10^{-4}$

38 ppm, respectively. It could be concluded that larger printing jobs for the same operating time might cause a higher frequency of evaporation of toner and/or fusing materials, subsequent nucleation and condensation into primary particles, and thus larger values of number decrease (or diameter increase) and mass emission rates were observed. A remarkably large amount of the emission at 38 ppm might have originated from a its operating character, a two-component system, which might contribute to the emission increase owing to a higher fusing temperature and easily detached fine additive particles on the toner surface. The results could provide an understanding of the emission trends of laser printers with different speeds and provide information on the emission control via pre- (*i.e.*, during printer development and manufacturing) or post-treatment (*i.e.*, during printer operation) concerns.

## References

- Anderson, J.H., 1996. The effect of additives on the tribocharging of electrophotographic toners. *Journal of Electrostatics* 37, 197.
- Bémer, D., Lecler, M.T., Régnier, R., Hecht, G., Gerber, J.M., 2002. Measuring the emission rate of an aerosol source placed in a ventilated room using a tracer gas: influence of particle wall deposition. *The Annals of Occupational Hygiene* 46, 347.
- Chen, C.-L., Chiu, G.T.-C., 2008. Halftone banding reduction for a class of electrophotographic system-part II: closed-loop control. *Mechatronics* 18, 412.
- Gudmundsson, A., Löndahl, J., Bohgard, M., 2007. Methodology for identifying particle sources in indoor environment. *Journal of Environmental Monitoring* 9, 831.
- Hänninen, O., Bröske-Hohlfeld, I., Loh, M., Stoeger, T., Kreyling, W., Schmid, O., Peters, A., 2010. Occupational and consumer risk estimates for nanoparticles emitted by laser printers. *Journal of Nanoparticle Research* 12, 91.
- He, C., Morawska, L., Taplin, L., 2007. Particle emission characteristics of office printers. *Environmental Science and Technology* 41, 6039.
- Hinds, W.C., 1999. *Aerosol Technology*. John Wiley and Sons, New York.
- Kagi, N., Fujii, S., Horiba, Y., Namiki, N., Ohtani, Y., Emi, H., Tamura, H., Kim, Y.S., 2007. Indoor air quality for chemical and ultrafine particle contaminants from printers. *Building and Environment* 42, 1949.
- Kim, S.-Y., Kim, Y., Byeon, J.H., Lee, D.-Y., Hwang, J., 2009. Emission of submicron aerosol particles in operating a laser beam printer. *International Journal of Precision Engineering and Manufacturing* 10, 33.
- Lee, S.C., Lam, S., Fai, H.K., 2001. Characterization of VOCs, ozone, and PM10 emissions from office equipment in an environmental chamber. *Building and Environment* 36, 837.
- Mio, H., Higuchi, R., Ishimaru, W., Shimosaka, A., Shirakawa, Y., Hidaka, J., 2009. Effect of paddle speed on particle mixing behavior in electrophotographic system by parallel discrete element method. *Advanced Powder Technology* 20, 406.
- Pettersson, T., Fogden, A., 2006. Leveling during toner fusing: effects on surface roughness and gloss of printed paper. *Journal Imaging Science and Technology* 50, 202.
- Ramesh, P., 2009. Modeling and control of toner material state in two component development systems. *Journal of Imaging Science and Technology* 53, 041206.
- Schripp, T., Wensing, M., Uhde, E., Salthammer, T., He, C., Morawska, L., 2008. Evaluation of ultrafine particle emission from laser printers using emission test chambers. *Environmental Science and Technology* 42, 4338.
- Seipenbusch, M., Binder, A., Kasper, G., 2008. Temporal evolution of nanoparticle aerosols in workplace exposure. *The Annals of Occupational Hygiene* 52, 707.
- Virtanen, A., Ristimäki, J., Keskinen, J., 2004. Method for measuring effective density and fractal dimension of aerosol agglomerates. *Aerosol Science and Technology* 38, 437.
- Wensing, M., Schripp, T., Uhde, E., Salthammer, T., 2008. Ultra-fine particles release from hardcopy devices: sources, real-room measurements and efficiency of filter accessories. *Science of the Total Environment* 407, 418.